Egypt. J. Chem. **Vol. 64,** No. 7 pp. 3335 - 3349 (2021)

Egyptian Journal of Chemistry

http://ejchem.journals.ekb.eg/

Tailoring Nano-Copolymer/CNTs Composite and its Application in Drug Delivery

M. K. Darwish[a*], Mohamed Shaban[b,c], R.A. Sobh[d], A. A. Abdel Khalek[a]

[a] *Chemistry Department, Faculty of Science, Beni-Suef University, Beni-Suef, Egypt*
[b] *Nanophotonics and Applications Lab, Physics Department, Faculty of Science, Beni-Suef University, Beni-Suef 62514, Egypt*
[c] *Physics Department, Faculty of Science, Islamic University of Madinah, P. O. Box: 170, AlMadinah Almonawara 42351, Saudi Arabia*
[d] *Polymer and Pigment Department, National Research Centre, Giza, Egypt*

Abstract

This work aimed to overcome the main drawbacks of some essential anticancer drugs as 5-Fluorouracil (5-FU) by controlled loading with novel drug carriers. By a differential microemulsion technique, nanosized particles derived from a copolymer of poly(methyl methacrylate (MMA) and 2-hydroxyethyl methacrylate (HEMA)) with different monomer ratios have been synthesized and used as a drug carrier. Poly(MMA-co-HEMA)/MWCNT nanocomposite was also synthesized using an in-situ microemulsion polymerization technique and used as a 5-FU carrier. Different techniques have characterized these ground-breaking drug delivery systems such as FT-IR, XRD, TEM, TGA, zeta potential, and a particle size analyzer. The effects of monomer feed composition, 5-FU content, and MWCNTs content on morphological and structural properties, in-vitro 5-FU release, and entrapment efficiency (EE%) have been studied. It was noted that the inclusion of MWCNTs in the 5-FU-loaded polymer increases the thermal stability and raises the entrapment efficiency (EE%) to hit 99% at CNTs:5-FU ratio of 2:1. The anticancer drug release from the co-polymeric nanospheres depends on the HEMA ratio, 5-FU/copolymer ratio, CNT/5-FU ratio, and the pH of the medium. The optimized nanocomposite demonstrated higher anti-tumor activity against the cell lines CaCo-2, MCF-7, and HepG-2 and higher cytotoxicity against HepG-2 relative to CaCo-2 and MCF-7.

Keywords*:* MWCNTs/polymer nanocomposite; 5- fluorouracil; microemulsion polymerization; methyl methacrylate; 2-hydroxyethyl methacrylate; drug delivery systems.

Introduction

The development of novel drug delivery systems is imported for improving the pharmacological profiles of several classes of therapeutic molecules and overcoming the drawbacks associated with some essential drugs. As an anti-cancer drug, 5-FU can achieve effective drug therapy with minimal side effects [1]. This could be achieved by incorporating the drug into a novel carrier which could increase its oral bioavailability and prolong its duration of action.

The microemulsion system is the most efficient drug delivery system, which demonstrates high efficiency of drug trapping, release under a sunken environment, biodegradability, and easy removal from the body [2,3]. The microemulsion technique can produce polymer latexes with particle sizes lower than 50 nm, low viscosity, and wide temperature range stability [4,5]. In situ microemulsion polymerization is considered to be an effective method in drug entrapment during the formation of polymer nanosphere [6-8]. In the drug delivery application, CNTs were used due to their hollow nanostructures and fantastic physicochemical features [9-12]. CNTs are also highly capable of entering biological cells without injury, but their use in pharmacology is limited by the low dispersion of CNTs in aqueous solutions. The modification of CNTs could therefore increase their selective distributions, control the release of the drug, act as an active compartment in increasing the cytotoxicity [13]. MWCNT can be functionalized with polymers to produce MWCNT/polymer nanocomposites with special

*Corresponding author e-mail: mohamed.darwish88@yahoo.com.; (Mohamed K. Darwish).
Receive Date: 31 January 2021, Revise Date: 02 March 2021, Accept Date: 14 March 2021
DOI: 10.21608/EJCHEM.2021.60541.3303

functions and high biocompatibility [14]. Entezar-Almahdi et al. reported that the MWCNTs functionalization is obligatory to improve their preoccupation and bioavailability [15]. Also, González-Lavado et al. demonstrated that the use of MWCNTs as a drug delivery system improves the efficiency of used chemotherapy drugs [16].

5-FU is the most commonly used anticancer drug in chemotherapy treatment; however, it inhibits the growth of normal body cells and often induces many side effects like other chemotherapy drugs [17]. The 5-FU treatment rate is less than 15 percent due to its poor bioavailability. Furthermore, 5-FU produces major toxicological damages to the blood and gastrointestinal system [18,19]. So, to realize a stronger treatment with fewer side effects, it is important to establish a hopeful drug delivery system for 5-FU. Entezar-Almahdi et al. summarized the recent Advances in designing 5-FU delivery systems [20]. It was suggested that the loading of the drug into MWCNTs/polymer nanocomposite will be effective in improving its efficiency and reducing the side effects caused by the application of the free drug. However, to the best of our knowledge, there is no detailed report on the implementation of the 5-FU drug delivery utilizing the MWCNT/poly(MMA-co-HEMA) system.

This work aimed to synthesize poly(MMA-co-HEMA) with varied monomer ratios and MWCNT/poly(MMA-co-HEMA) nanocomposites and trap them with the 5-FU drug-using differential microemulsion copolymerization method. The polyvinyl pyrrolidone (PVP) was used as a biocompatible emulsifier to produce nanoparticles (NPs) and prevent coagulation. The effects of the MMA/HEMA ratio, 5-FU/copolymer ratio, CNT/5-FU ratio, and the pH of the medium on the colloidal properties and drug delivery performance of the designed carriers have been studied. Zeta potential, thermal stability, drug capture performance, in vitro drug release, and in vitro anti-tumor cytotoxicity against CaCo-2, MCF-7, and HepG-2 cell lines have been also investigated.

Materials and methods

Materials

MMA and HEMA were purchased from Sigma Aldrich Company(Germany) and used after purification utilizing active Al2O3 and SiO2 gel columns [21]. The purified MMA and HEMA were preserved in dark containers in a refrigerator for use within four weeks. PVP (Bioshop, Canada), (NH4)2S2O8 (APS, Sigma Aldrich, Germany), 5-FU drug (Biobasic Canada Inc.) were used as purchased. MWCNTs were prepared in our NPA Lab [22, 23]. C2H6O, HCl, KCl, and NaOH were obtained from El-Nasr Company (Egypt). HNO3 and H2SO4 were obtained from Nen Tech Ltd (UK). KH2PO4 was bought from GenLab (Egypt).

Experimental procedures

Modification of MWCNTs

MWCNTs were dissolved in HCL (Dil.) with concentration (5%) and stirred with a magnetic stirrer for 30 min (add CNTs gradually not at one time to make sure reaction occurs) there would be effervescence during addition. MWCNTs were filtered using Buchner and collected carefully in a glass bitter dish for drying in an oven at 80° C for 18 hr. Then MWCNTs were dissolved in 1 H2SO4: 3 HNO3 and refluxed for 4 hr at 120° C to get rid of catalyst and open limbs of MWCNTs. Dilution was done by distilled water over the mixture of MWCNTs, H2SO4, and HNO3, then filtration was done and washing with distilled water for 10 times and the product was dried in the dryer at 100°C for 12 hr.

Preparation of the nano-polymeric material

Poly(MMA-co-HEMA) of different monomers ratios were designed through a microemulsion having a 10% monomers mixture, PVP as an emulsifier, and APS as initiator. The copolymerization reaction was performed in a three-necked flask (250 ml) provided with a condenser and two funnels. Mechanical stirring was carried out at 350 rpm in a water bath with a temperature controller. The microemulsion polymerization process included the following steps [24]: The PVP is dissolved in 30 ml of deionized (DI)-H2O in a flask using a mechanical stirrer and then left at room temperature overnight. The APS is then dissolved in 15 mL DI-H2O in a beaker. 30% of this APS solution is added to the PVP solution and left in H2O bath at 65oC to throw out the dissolved O2. When the temperature reaches the initiator's decomposition temperature (65oC), the required concentration of the monomers, as well as 60% of the APS solution, dropped wisely added to the aqueous phase via the dropping funnel over 1 h. After the

addition of the rest 10% of APS solution, the solution was left for another 2 h to complete the polymerization.

Synthesis of 5-FU-loaded MWCNTs/copolymer nanocomposites

The 5-FU-loaded poly(MMA-co-HEMA)/MWNTs nanocomposites were synthesized using the in-situ microemulsion polymerization technique [25, 26]. The weighed amount of the functionalized MWNT was added to the emulsifier's aqueous solution and exposed to ultrasound for 10 min. Then, the 5-FU was added to this aqueous solution in the three-necked flask. The weighted APS was applied to 15 ml DI-H2O and the initiator solution wisely fell through the funnel along with the monomers to begin the polymerization that lasted up to 2 hours until the monomer odor is gone.

Samples characterization

Morphology and particle size

A transmission electron microscope (TEM, JEM-1230) operating at 60 kV was used to analyze the morphology of the MWCNTs, copolymers, and nanocomposites. The samples were diluted with DI-H2O not less than 10 times before taking the TEM images. A well-distributed drop of the diluted sample is loaded on a copper grid and dried at room temperature. H3PW12O40 (0.4 %) drop is used as a stain for the dried sample.

Zeta potential characterization

Malvern ZetaSizer (3000-HS) is used to measure the electrophoretic mobilities (με) of the designed nanostructures. Using Smoluchowski's equation, the zeta potential (ζ) is obtained [27].

$$\zeta = \eta/\varepsilon \times \mu e \qquad (1)$$

Here ε and η refer to the medium permittivity and viscosity, respectively. Triplicate measurements were carried out and the average values were recorded.

Thermogravimetric analysis

The thermogravimetric analysis (TGA) was carried out for the pure 5-FU, free (MMA/HEMA50/50) copolymer, 5-FU/(MMA/HEMA50/50) copolymeric nanoparticle, and 5-FU/MWCNTs/copolymer nanocomposite. Where samples of 5 mg were put on a Pt thin pan and the measurements were carried out under purging of nitrogen @10 oC.min-1 heat flowrate [28]. The temperature is ranged from 30 to 600oC.

Structural properties and Function groups

X-ray diffraction (XRD) charts of pure 5-FU, free copolymer (MMA/HEMA50/50), 5-FU/(MMA/HEMA50/50) copolymer NPs, and 5-FU/MWCNTs/copolymer nanocomposite were measured using a Bruker/Siemens D5000 diffractometer (λ=1.54Å). The XRD charts were measured at 40 mA current and 45 kV potential from 10° to 80° with scan rate 4o/min. Fourier transform infrared spectroscopy (FTIR) was used to identify the functional groups and vibrational modes of 5-FU, PMMA/HEMA50/50, 5-FU-loaded PMMA/HEMA50/50 NPs, and 5-FU-loaded polymer/MWCNTs nanocomposite. The FTIR spectra were measured via Perkin Elmer IR spectrophotometer from 400 to 4000 cm-1 at 4 cm-1 steps for disks composed of 2 mg sample/200 mg KBr [29].

Drug delivery and Cytotoxicity

Drug Entrapment Efficiency (EE)

The EE of the drug for the copolymer NPs and MWCNTs/copolymer nanocomposite was calculated by determining the free drug using an indirect method, as follows [30]:

The free drug was separated from polymeric NPs and the nanocomposite by dissolving in methanol where the polymeric NPs are suspended in methanol, and then they separated from the polymeric NPs by refrigerated ultracentrifugation with 50000 rpm for 0.5h. The concentrations of the free drug in the supernatant solutions were quantitatively analyzed by a double beam UV spectrophotometer at the specified wavelength (λmax= 266 nm) after measuring a series of known concentrations of the drugs to draw the calibration curve.

The values of EE were calculated from equation (2) using the actual weight of the drug in the sample and the initial or theoretical weight of the used drug [31, 32].

$$\text{Entrapment Efficiency} = \frac{\text{actual weight of the drug in sample}}{\text{theoretical weight of the drug}} \times 100 \qquad (2)$$

In-vitro 5-FU release

The in-vitro 5-FU drug release from copolymer NPs and MWCNTs/copolymer nanocomposites were carried out in simulated intestinal solution (pH 7.4)

and gastric solution (pH 1.2) via the dialysis bag method [26, 33]. The buffered saline fluid with pH 7.4 was obtained by adding 0.250 liter of 0.1 M potassium dihydrogen phosphate and 0.195 liter of 0.1M sodium hydroxide pellets. While the buffered saline with pH 1.2 was obtained by adding 0.250 liter of 0.2 M hydrochloric acid to 0.147 liter of 0.2M potassium chloride. The dialysis bag was equilibrated before the experiment with the buffer fluid for a few hours [8]. 500 mg of the 5-FU-loaded copolymeric nanocomposite was added to 5 ml of the buffer fluid, placed in the dialysis bag, and then immersed into a closed vessel having 0.1litre of the buffer @100 rpm stirring and 37°C ± 0.5°C [34]. 5 ml of the sample was withdrawn after regular interval times to carry out the 5-FU release analysis and compensated with an equivalent amount of fresh buffer to preserve the condition of sinking. The samples will be analyzed for drug content using a calibration curve for the drug in each buffer solution by UV spectrophotometer at λmax for 5-FU.

The drug release percent was calculated by equation (3);

$$\text{Release (\%)} = \frac{\text{Released drug (5FU)} \times 100}{\text{Total drug (5FU)}} \qquad (3)$$

Cytotoxicity assay

The cytotoxicity of 5-FU-loaded MWCNTs/ polymer nanocomposite was measured using the technique of tissue culture. HepG-2 (hepatocellular carcinoma), MCF-7 (breast cancer), and CaCo-2 (human colorectal adenocarcinoma) cell lines were delivered from the Pharmacology Unit, National Cancer Institute, Cairo University, Egypt. They were held at 37ºC and 5% CO2 in DMEM media of 10% fetal calf serum, sodium pyruvate, 100 U/ml penicillin, and 100 mg/ml streptomycin until the bioassay of cytotoxicity was performed. The cytotoxicity of the sample was evaluated using Skehan et al. process [35]. Generally, during the night afore applying the prepared samples, we put 100 cells/well on 96-well plates to enable cells to be attached to the walls of the plate. We added diverse concentrations of the examined sample (2.5, 5, 10, 20, 40, 80, 160, 320, 625, 1250, 2500, 50000 µg/ml) to a monolayer cell. For each dosage, triple wells are used. Monolayer cells are protected at 37oC and 5 percent CO2 with the analyzed agents for 2 days. At the end of the incubation cycle, the cells are fixed and marked with C27H30N2O7S2 dissolved in CH_3 COOH. The unattached stains are detached thru a four-times wash process using 1% CH_3 COOH. A Tris-EDTA buffer is used to collect the proteins-bound dyes. The absorption is determined in ELISA readers. Three independent trials are accomplished in triplicates. The values of viability% are plotted versus the sample concentrations to obtain the survival curves of the studied tumor cell lines. The values of half-maximal inhibitory concentration (IC50) are estimated from the survival curve for the various pre-mentioned cell lines.

Results and discussions

Modification of MWCNTs

MWCNTs were functionalized and purified by an acidified oxidation process to eliminate the amorphous carbon and catalyst. In the form of the -COOH group, the purified CNT contains oxidizing carbon. CNTs were pre-treated through sonication in an acidic medium and then refluxed for reducing their chain length and generating carboxylic groups that increase their dispersibility [36].

Figure 1 displays the FTIR spectra for CNTs afore and after functionalization. It was noted from FTIR spectra that the featured modes of [-C=O-], [-C-O], and [-OH] groups for the functionalized CNT appeared more intense than the CNTs before functionalization. Where, the stretching vibrations of -C-O, -C=O-, and -OH bands appeared clearly at (1036, 1112), (1571, 1636), and 3435 cm-1, respectively.

Figure 2 shows TEM images for both pristine and functionalized MWCNTs. Many un functionalized MWCNTs are found to accumulate together to form a wide domain of bundles because of the powerful Van der Waals forces and interference of MWCNTs with each other. TEM images of Figure 2 show that the diameter of functionalized MWCNTs increased relative to the diameter of pristine MWCNTs because of the existing function groups on the functionalized MWCNTs surfaces. Before functionalization, the inner and outer diameters were 4.4 and 8.1 nm respectively. After functionalization, the outer diameter of MWCNTs is increased to 17.9 nm.

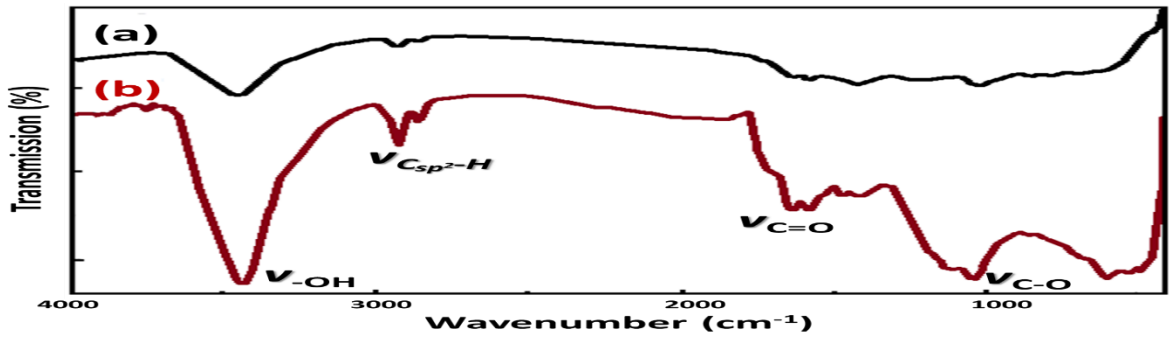

Figure 1: FTIR spectra for CNTs (a) afore and (b) after functionalization.

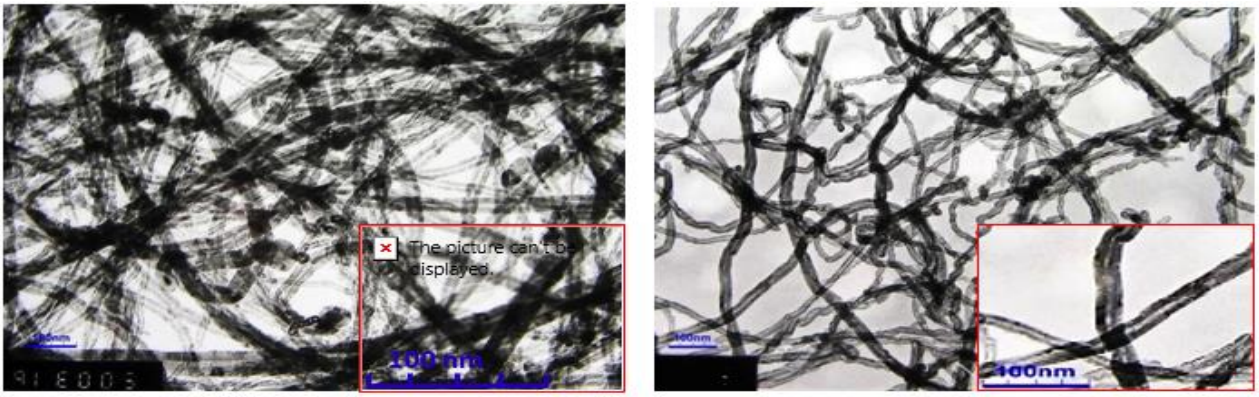

Figure 2: TEM images of MWCNTs (a) afore and (b) after functionalization

Morphological examination of MMA/HEMA and CNTs/ MMA/HEMA

Effect of MMA/HEMA monomer feed composition

The effect of the MMA/HEMA ratio on the morphology of the formed 5-FU loaded polymeric nanospheres was demonstrated in Figure 3. As the monomer feed ratio increases, the particle size is increased. At MMA/HEMA monomer feed ratio of 90/10, Fig.3A, the diameter of the polymeric nanospheres is ranged from 83 to 97.5 with an average value of 97.5 ± 14 nm. At the feed ratio of 70/30, Figure 3B, the average value of the polymeric nanospheres diameter is increased to 143± 13 nm. From Figure 3C, the average value of the polymeric nanospheres diameter is increased to 187± 14 nm @ 50/50 MMA/HEMA monomer feed ratio. It has been observed from Figure 3 that as the monomer feed ratio increased, the polymer nanospheres could be loaded with high 5-FU drug content to form core-shell (polymer nanosphere/5-FU) morphology as shown in the inset of Figure 3C. The thickness of the shell was 35 ±3 nm.

Effect of drug content

Figure 4 shows TEM images of 5-FU/copolymeric NPs as a function of the drug to MMA/HEMA (70/30) copolymer ratio; 1:20(A), 1:10(B), and 1:6(C). It has been observed from Figure 4 that the rise of the drug content from 1:20 to 1:6 leading to an increase in the particle size from 143± 13 nm to 177± 10. It is observed from the inset images of Fig.4 that a shell of increased thickness is grown around the polymer nanospheres. As the drug content increased from 1:10 to 1:6, the shell thickness is increased from 23.3± 3.5 nm to 38.9± 6.1 nm. This means that 5-FU could be loaded with high drug content into the polymer nanospheres for a drug to a monomer ratio of 1:6.

Effect of CNT loading

Figure 5 shows the TEM micrographs of (A) 5-FU-loaded MMA/HEMA (50/50) copolymer and (B) 5-FU-loaded MWCNTs/(MMA/HEMA 50/50) nanocomposite with 5-FU/MWCNTs ratio of 1:1. In Figure 5A, a core (polymeric nanosphere)-shell(5-FU) morphology is observed. The TEM image of 5-FU/ polymeric/CNTs indicates that the introduction of

CNTs within the polymer matrix causing morphological changes., Figure 5B This image refers to the effective intercalation of polymer and MWCNTs within nanospheres [3, 6]. CNTs of spherical aggregates with an average diameter of 36.0 ± 4.9 nm surrounded polymeric nanospheres of an average diameter of 290.8 ± 36.1 nm. Also, many 5-FU spherical NPs with an average diameter of 152.1 ± 17.7 nm are growing around the CNTs/polymeric spheres. This is an indication of the binding of many 5-FU NPs to one CNTs/polymeric NPs.

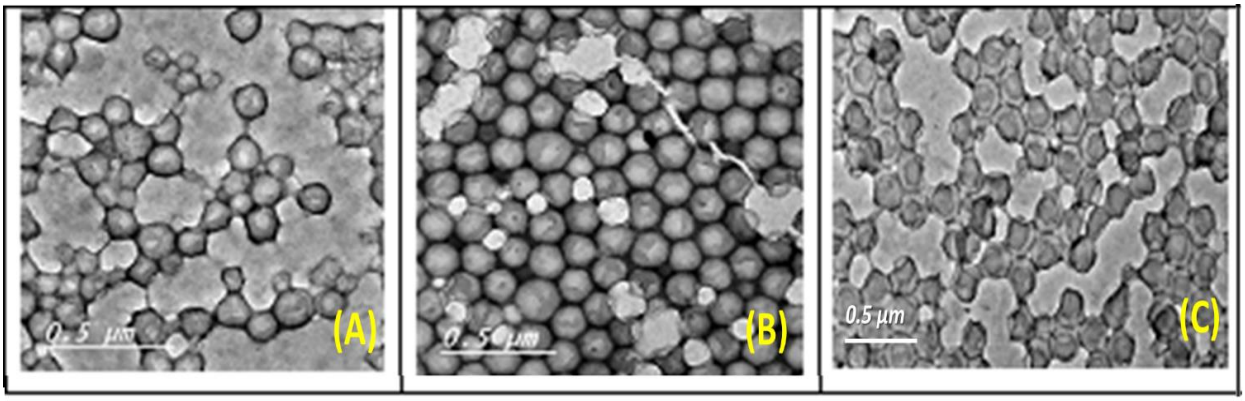

Figure 3: TEM images of 5-FU-loaded copolymeric nanospheres of different MMA/HEMA ratios; 90/10(A), 70/30(B), and 50/50(C).

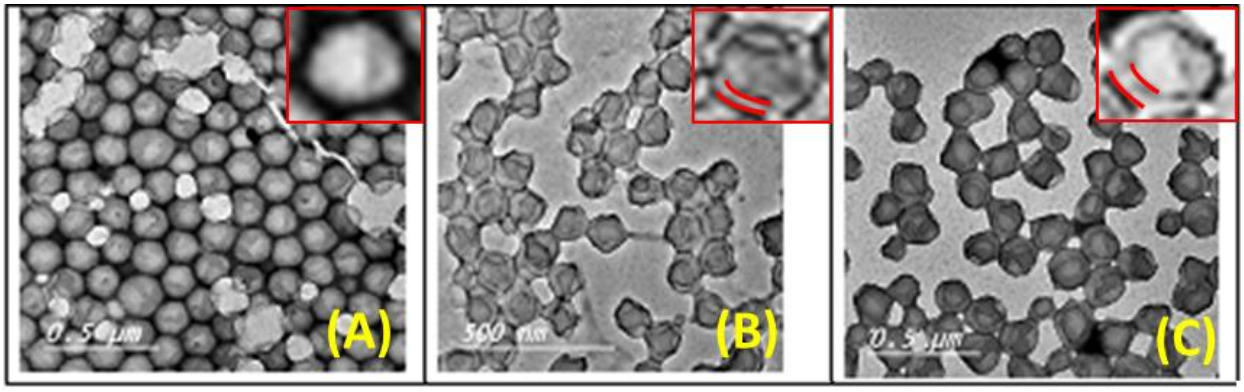

Figure 4: TEM images of 5-FU/copolymeric NPs with different drug to MMA/HEMA(70/30) copolymer ratios; (A)1:20 (B) 1:10 (C) 1:6.

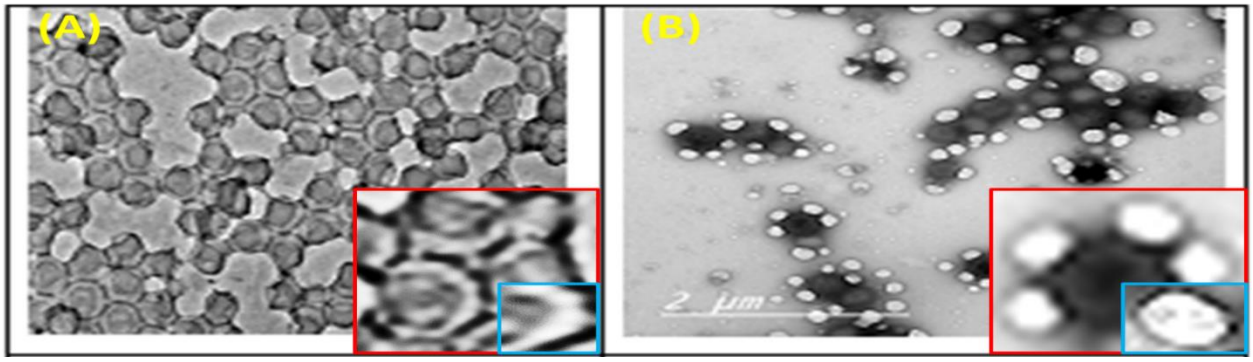

Figure 5. TEM micrographs of (A) 5-FU loaded-polymer nanosphere with monomer feed compositions (50/50) and (B) 5-FU-loaded MWCNTs/(MMA/HEMA(50/50)) copolymer nanocomposite with 5-FU/MWCNTs ratio of 1:1.

Zeta potential and particle size

The zeta potential was used as a measure of the colloidal stability of the nanoparticle suspension where it was considered as an indicator of the magnitude of electrostatic interaction between colloidal particles. The increase in zeta potential provided good stability against coagulation in the colloid system. The data presented in Table 1 showed low negative zeta potential of the prepared microemulsion lattices and this means that the formed latex is stable. But with increasing the HEMA ratio in the latex, the zeta potential value (ζ) increases from -0.39 mV to -0.6 mV due to the increase in the surface charge with the existence of additional hydroxyl groups in the repeated units [37]. The particle size measurements, Table 1, also show the increase of the particle size from 70 nm to 150 nm as the composition of the MMA/HEMA monomer feed is altered from 90/10 to 50/50. This implies that the particle size is duplicated by increasing the content of HEMA, which is well in line with the particle size found by TEM analysis, Figure 3. Also, the average values of the particle size of the NPs obtained with different drug/MMA/HEMA (70/30)-copolymer ratios (1:20, 1:10, and 1:6) are presented in Table 1. The size of the nanoparticle was found to increase as the 5-FU content increased, whereas the particle size increased from 85 to 105 and 120 nm by changing the Drug/ (70/30) copolymer ratio from 1/20 to 1/10 and 1/6, respectively. This indicated that the drug was well loaded into the polymeric NPs as observed in Figure 4.

The value of ζ for 5-FU-loaded MWCNTs/(MMA/HEMA50/50) nanocomposite is -1.34 mV. This means that the incorporation of functionalized MWCNTs shifts the zeta potential from -0.6 to -1.34 mV, which results from the existence of the carboxylic groups after the acidic functionalization of the MWCNTs [7, 8]. The particle size measurements, Table 1, also show the increase of the particle size from 150 nm to 240 nm by the incorporation of CNTs to form 5-FU loaded-MWCNTs/copolymeric(50/50) nanocomposite with 5-FU/MWCNTs ratio of 1:1. This implies the increase of the particle size by a 1.6 factor, which agrees well with the particle size found by TEM analysis, Figure 5.

1. Effect of MMA/HEMA ratio on ζ and Dv of drug-loaded copolymer NPs			
MMA/HEMA	90/10	70/30	50/50
Zeta Potential (mV)	-0.39	-0.42	-0.6
Particle size Dv (nm)	70	85	150
2. Effect of drug/ (70/30) copolymer ratio on ζ and Dv of drug-loaded copolymer NPs			
5-FU Drug	1	1	1
MMA/HEMA(70/30) copolymer ratio	20	10	6
Particle size Dv (nm)	85	105	120
3. Effect of CNTs on ζ and Dv of 5-FU loaded-CNTs/copolymer(50/50) composite			
CNTs/drug ratio	0	1	
Zeta Potential (mV)	-0.6	-1.34	
Particle size Dv (nm)	150	240	

Table 1. Values of Zeta potential and particle size.

Thermal gravimetric analysis (TGA)

Figure 6A showed the TGA analysis of pure 5-FU, free copolymer (MMA/HEMA50/50), 5-FU-entrapped polymeric NPs, and 5-FU-loaded MWCNTs/copolymer nanocomposite. Table 2 presented the TGA values of these samples, where the temperatures at which the samples lose 20% and 50% of their original weights are T20% and T50%. In general, the thermal stability of the studied samples is in the order; drug-loaded copolymer (MMA/HEMA50/50) > free copolymer (MMA/HEMA50/50) > pure 5-FU. So, the drug-loaded polymer was more thermally stable than the free drug. The temperature required for the samples to lose 10% of their original weight was 187, 278, and 238oC for pure 5-FU, free copolymer (MMA/HEMA50/50), and 5-FU-entrapped polymeric nanoparticle. These temperatures were increased to 318, 368, and 395oC for the samples to lose 90% of their original weights. The expected released molecules are also presented in Table 2 at the specific temperatures.

Figure 6B showed TGA for 5-FU-loaded copolymer (MMA/HEMA50/50) relative to 5-FU-loaded MWCNTs/copolymer nanocomposites with CNTs/drug ratios of 1:2 and 2:1. Table 3 presented the TGA values of these samples. The TGA values, Table 3, showed that the 5-FU-loaded MWCNTs/copolymer nanocomposite is more

stable than the 5-FU-loaded copolymer (MMA/HEMA50/50). Also, it is noted that the thermal stability is increased with increasing MWCNTs/drug ratio from 1:2 to 2:1[10, 25].

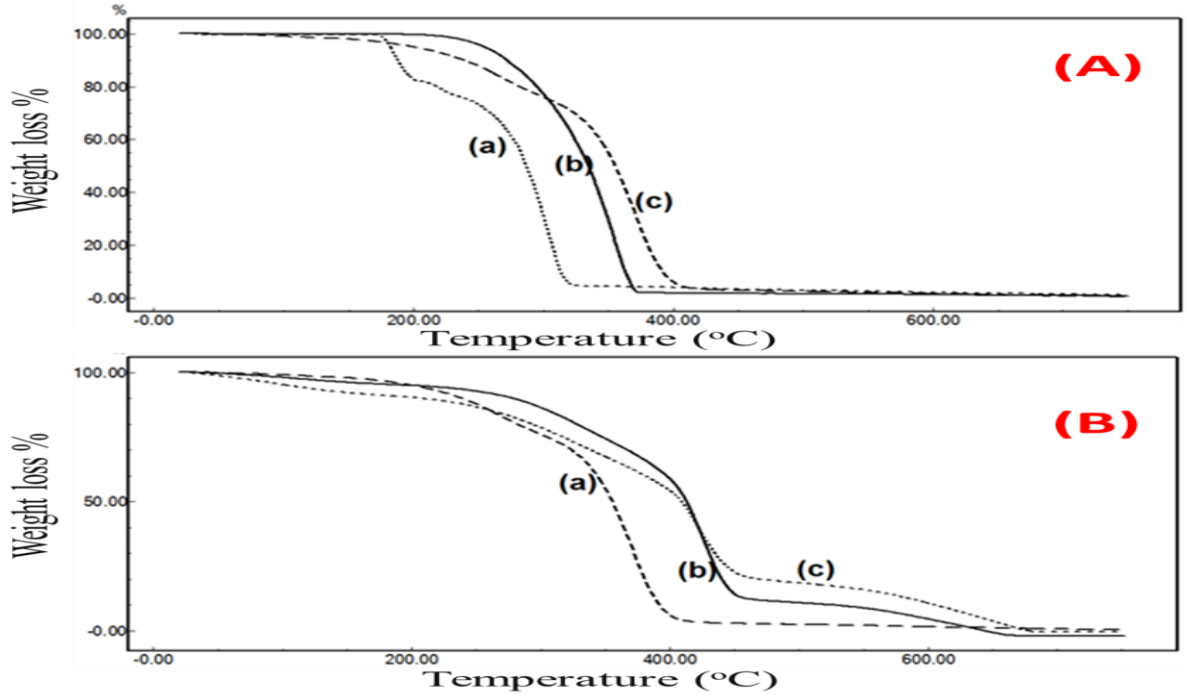

Figure 6. (A)TGA of (a) pure 5-FU, (b) free copolymer (MMA/HEMA50/50), and (c) 5-FU-entrapped copolymer nanoparticle; and (B) TGA of (a) 5-FU-loaded copolymer (MMA/HEMA50/50), 5-FU-loaded MWCNTs/copolymer nanocomposites with CNTs/drug ratios of (b) 1:2 and (c) 2:1.

Structural properties and function groups

XRD results

Figure 7 displays the observed and calculated XRD charts of 5-FU, PMMA/HEMA50/50 copolymer, 5-FU-loaded PMMA/HEMA50/50 NPs, and 5-FU-loaded MWCNTs/copolymer nanocomposite. From Figure 7i, it was clear that 5-FU is a polycrystalline material with numerous characteristic peaks. The 5-FU peaks are observed at 2θ of 16.46◦, 19.14◦, 20.82◦, 20.82◦, 22.02◦, 28.78◦, 32.18◦, and 33.46◦, suggesting its polycrystalline nature. The sharpest and highest one is observed at 28.78◦. The observed XRD pattern, Fig.7A(ii), of PMMA/HEMA50/50 exhibits abroad band companied with XRD peaks @ 2θ values of 13.49◦, 18.36◦, 20.48◦, 28.56°, 31.98° and 49.95° as observed from the calculated XRD pattern, Fig.7B(ii). This indicates the semi-crystalline nature of the copolymer. The XRD patterns of Figures 7A(iii) and

7B(iii) illustrated that the drug-loaded polymeric NPs have a decrease in peak intensity compared to pure copolymer due to the drug dispersed at the molecular level. The disappearance of some drug peaks and the reduction of the intensity of other peaks indicate the entrapment of the drug inside the polymer and also indicates the direction toward the disordered crystalline phase of the encapsulated drug [38]. For the 5-FU MWCNTs/copolymer, Figures 7A(iv) and 7B(iv), there was an additional peak at 2θ = 25.2° which was a characteristic peak along the (002) orientation of the pristine-CNTs [39]. Moreover, there was a further drop in peak intensity at ~ 21° and 29° which refers to a lesser detecting level of the encapsulated 5-FU due to the entrapment of 5-FU inside the MWCNTs/copolymer and the direction toward the amorphous nature of the encapsulated drug.

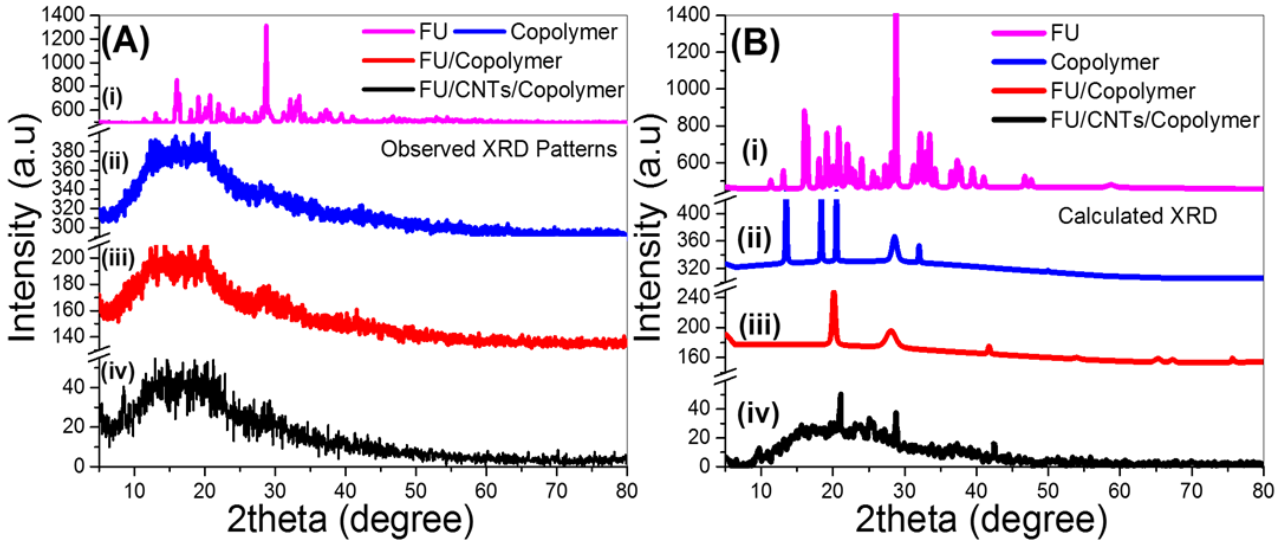

Figure 7. Observed (A) and (B) calculated X-ray diffraction patterns of (i) 5-FU, (ii) PMMA/HEMA50/50, (iii) 5-FU-loaded PMMA/HEMA50/50 NPs, and (iv) 5-FU-loaded polymer/MWCNTs nanocomposite.

FTIR analysis

Figure 8 shows the FTIR spectra of 5-FU, PMMA/HEMA50/50, 5-FU-loaded PMMA/HEMA50/50 NPs, and 5-FU-loaded MWCNTs/copolymer nanocomposite. The FTIR spectrum of 5-FU, Figure 8i, illustrated feature bands @3132–2825 cm−1 because of the C—H stretch modes. The bands @1428–1661 cm−1 referred to the C=N and C=C stretch modes. The band @ 1348 cm−1 has resulted from the vibrational mode of the pyrimidine compound. Also, the 1138 cm−1 and 1244 cm−1 modes have resulted from the C—O and C—N vibrations, correspondingly. Moreover, the bands @466–879cm−1 are due to the aromatic ring [40].

The FTIR spectrum of MMA-co-HEMA copolymer, Figure 8ii, showed strong vibrations @2952 and 1733 cm-1 because of aliphatic C-H and carbonyl C=O stretches in both MMA and HEMA units. Several modes are observed @1663–1283 cm-1 because of the CH3/CH2 deformations. The strong modes @1077 and 982 cm-1 are assigned to the asymmetric/symmetric vibrational modes of C-O-C, respectively. Strong bands at 3757cm-1 and 3436 cm-1 are assigned to the stretch modes of -OH and C-H, respectively. The bands that appeared at 1068 and 1283cm-1 were ascribed to the ester stretching vibration of acrylate polymer.

The FTIR spectrum of the drug-loaded copolymer, Figure 8iii, refers to the existence of both 5-FU and the copolymer. It showed the functional groups of HEMA -OH mode@3384 cm−1 and the -COOH mode of 5-FU @2946 cm−1 with higher intensity than that observed for free 5-FU. The modes@575 and 746 cm−1 are often due to the aromatic bending of C=C, which is observed in the free 5-FU FTIR spectrum but not observed in the free copolymer FTIR spectrum.

The 1719 cm−1 mode corresponds to the C=O of the drug, which suggests the encapsulation of 5-FU into the copolymer. The FTIR of 5-FU-loaded MWCNTs/copolymer nanocomposite is illustrated in Figure 8iv. The –C=O stretching mode is located at 1733.8 cm−1. The – CH3 and –CH2 stretching vibrations are located at 2930 cm−1. The strong mode at 1446.8 cm−1 is referred to –CH bending. The -C-O-C- ester stretching is observed at 1281.7– 1149.2 cm−1. The wideband at about 3424.4 cm-1 refers to the nanocomposite's -OH stretching.

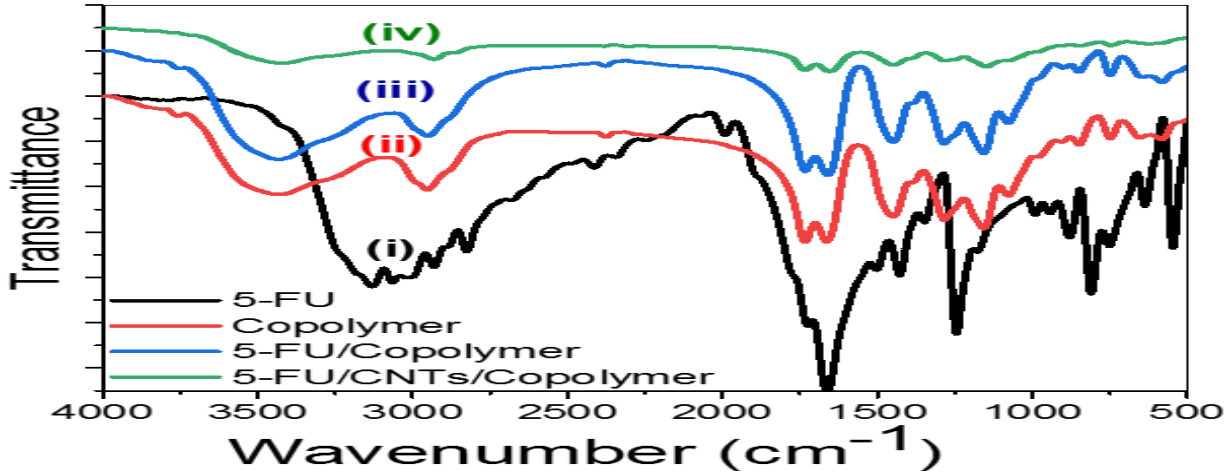

Figure 8. FTIR spectra of (i) 5-FU, (ii) PMMA/HEMA50/50 copolymer, (iii) 5-FU-loaded PMMA/HEMA50/50 copolymer NPs and (iv) 5-FU-loaded MWCNTs/copolymer nanocomposite.

Drug Delivery performance

Drug Entrapment Efficiency

The values of the drug entrapment efficiency (EE%) were estimated at different monomer feed composition, drug content, and MWCNTs content. The obtained values were presented in Table 2. In general, the EE% values are strongly dependent on monomer feed composition, drug content, and MWCNTs content as shown in Table 2. It was noted that drug EE% was influenced by the monomer feed composition. As the HEMA content increased, the EE% value is increased from 78% to 93% at 5% drug content. Also, the drug EE% is improved from 81% to 90% with increasing the drug content from 5% to 16.6%. Such data shows that by the differential microemulsion polymerization process, we can yield a 5-FU-loaded copolymer nanocomposite with high EE%. Moreover, as seen in Table 2, the EE% is significantly enhanced when the drug is loaded on the MWCNTs/(MMA/HEMA50:50) copolymeric nanocomposite. EE% reached about 99% @ high MWCNTs/drug ratio (2:1). Due to the drug's contact with MWCNTs/copolymer or filling in the inner cavities of the MWCNTs, the integration of MWCNTs into the copolymeric nanocomposite enables packing of higher 5-FU content [41]. the entrapment of 5-FU shows high values in the range of 94-99 % by comparing with the results of Masloub, Shaimaa M., et al [37]. where they incorporated 5-FU drug with PLGA polymer in microspheres and reached to the best condition of EE of 93.5 at high drug contents and the results of Sobh, R. A., et al [26]. in which the EE for 5-fluorouracil reached to 70% for 5-fu loaded Chitosan/MWCNT nanocomposite.

In Vitro Drug Release Studies

As a function of several variables including MMA/HEMA ratio, pH value, 5-FU, and MWCNTs contents, the release behaviors of the 5-FU are measured and presented in Figure 9. In general, the 5-FU drug release from the designed carriers indicates an initial blast effect, followed by a regulated release of the 5-FU as seen in Figure 9.

Effect of MMA/HEMA monomer feed composition

Figure 9(A, B) shows the drug release–time behaviors of MMA/HEMA copolymerize nanosphere system with different MMA/HEMA ratios (90/10, 70/30, 50/50) in simulated gastric and intestinal fluids @ pH 1.2 and 7.4, respectively. Using the copolymer (MMA/HEMA 50/50), The release of the 5-FU@ pH

7.4 is better than the release of 5-FU@ pH 1.2. Also, it was noted from this figure that the drug release rate of copolymeric (MMA/HEMA50/50) NPs was faster than that of the MMA/HEMA70/30 and MMA/HEMA90/10 copolymers. This may be ascribed to the higher hydrophilic nature of the copolymer (50/50) relative to the copolymers 70/30 and 90/10, as a result of the existence of additional hydroxyl groups in the repeated units [42]. A more hydrophilic copolymer would lead to faster ingestion of aqueous solution, resulting in quick rates of 5-FU dissolutions [27].

A	Effect of monomer feed composition	MMA/HEMA	90/10	70/30	50/50
		E. E. %	78	81	93
B	Effect of Drug content	Drug: Copolymer ratio (70:30) (Drug/copolymer%)	1:20 (5%)	1:10 (10%)	1:6 (16.6%)
		E. E. %	81	85	90
C	Effect of MWCNTs content	CNTs: drug	1:2	1:1	2:1
		E. E. %	94	97	99

Table 2. Values of EE% of 5-FU at different (A) monomer feed compositions @ 5%drug content, (B) drug content in the copolymer(MMA/HEMA70:30); and (C) MWCNTs content in the MWCNTs/copolymer (50:50) nanocomposite @ 5%drug content.

Influence of the pH value

The behavior of the drug release from the copolymer is studied using buffer solutions with pH values of 7.4 and 1.2, which simulated the intestinal and gastric fluids, Figure 9(C). Overall, because of the weakly bounded 5-FU to the wide surface area of the NPs, the release profiles in Figure 9(C) indicate quick starting release [37]. Also, it was noted that the release rates in the simulated intestine fluid, pH7.4, reached higher values compared to the simulated gastric fluid, pH 1.2. The drug release rates reached ~70%@pH 1.2 and 85%@pH 7.4 after 2h using the copolymer (50/50). The copolymer will then release fewer doses of the 5-FU drug in the stomach than in the intestine. However, the small difference in the copolymer release rates at pH 1.2 and pH 7.4 showed that the 5-FU-loaded copolymer can be applied at a wide variety of pH values.

Effect of drug content and MWCNTs content

The drug release rates were tested at different drug/copolymer ratios (1:20, 1:10, and 1:6) for the copolymeric MMA/HEMA 50/50 nanospheres, Figure 9(D). It was noted that the copolymer with higher drug loading is faster than that with lower drug loading because the higher drug loading in the nanospheres indicated a lower polymer matrix content, which facilitates drug dissolution from the nanospheres [2]. The drug release rates reached ~ 85% after 2h using drug: copolymer ratios (1:6) more than Masloub, Shaimaa M., et al [37]. Which reached to 70 % at high drug: PLGA polymer ratio (1:5).

From Figure 9(E), The 5-FU drug release rate from MWCNTs/copolymer nanocomposite is lower than the release rate from the pure copolymer @ pH 7.4. This can be ascribed to the encapsulation of 5-FU into the MWCNTs' internal cavities [43]. The increase of MWCNT relative to the 5-FU drug could improve the controlling of the 5-FU release [41].

In vitro Anti-tumor Cytotoxicity

The cytotoxicity of the sample was evaluated using Skehan et al. process [35]. The 5-FU-loaded MWCNTs/copolymer nanocomposite exhibited anti-tumor cytotoxicity against all examined cell lines. Figures 10(A-C) illustrated the variation of the viability percent versus the sample concentrations of the studied tumor cell lines (CaCo-2, MCF-7, HepG-2). As the concentration increases, the viability percent is reduced. The IC50 values are achieved via the measured concentrations for the investigated cell lines. The investigated sample showed the most significant effects versus the examined cell lines with IC50 of 1552 µg/ml for CaCo-2, 1420 µg/ml for MCF-7, and 78.7 µg/ml against HepG-2 (Figure 10(D)). The tested sample exhibited greater cytotoxicity with the HepG-2 cell line than with the other two cell lines.

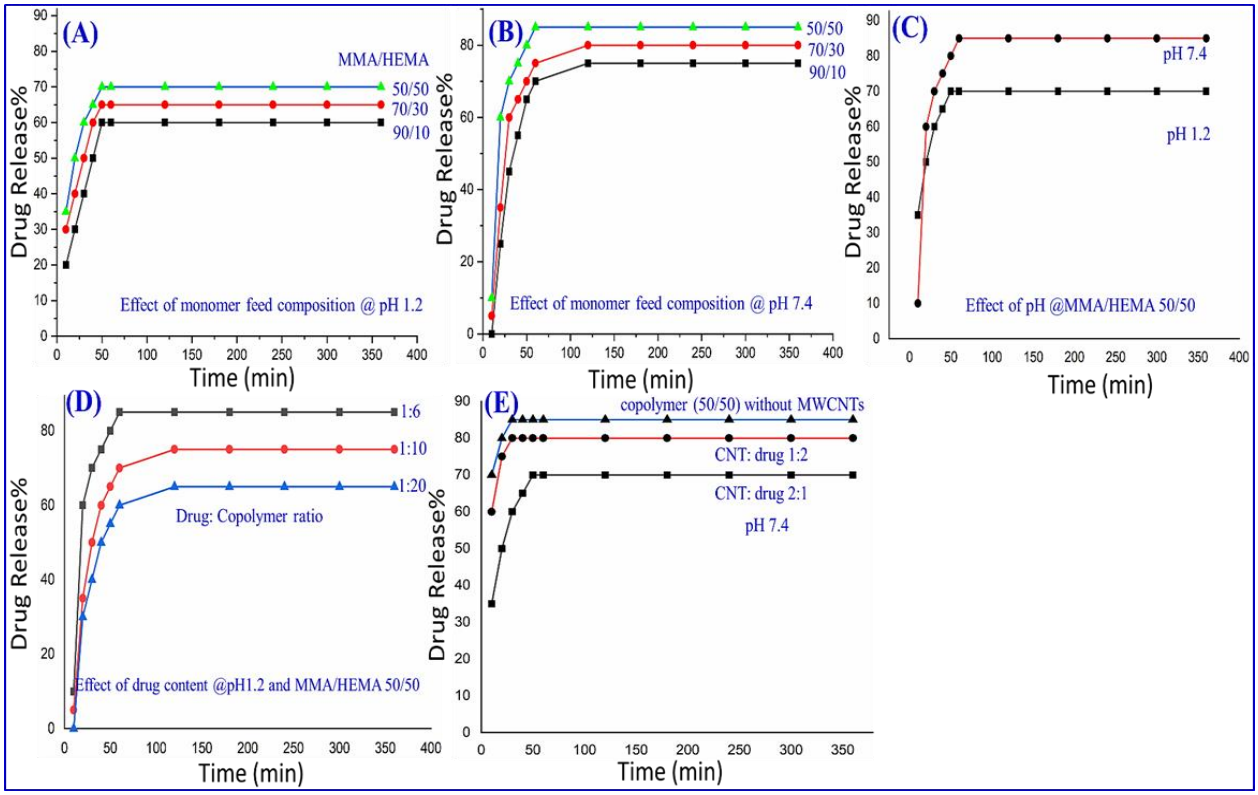

Figure 9. The 5-FU release profiles from copolymer NPs of diverse MMA/HEMA ratios (90/10, 70/30, 50/50) in simulated (A) gastric solution @pH 1.2 and (B) intestinal solution @pH 7.4; (C) from copolymer (50/50) at pH 7.4 and 1.2; (D) from copolymer (50/50) at pH 1.2 and different drug: copolymer ratios (1:20, 1:10, 1:6); and (E) from MWCNTs/copolymer(50/50) nanocomposite at pH 7.4 of different MWCNTs/drug ratios (1:2, 2:1) relative to the copolymer (50/50).

Conclusion

Using in-situ microemulsion polymerization techniques, methyl methacrylate/hydroxyl ethyl methacrylate (MMA/HEMA) copolymer and MMA-co-HEMA/MWCNTs composite NPs of various monomer feed compositions and CNT content have been synthesized and used as a 5-FU drug carrier. These revolutionary drug delivery systems have been characterized by different techniques including FTIR, XRD, TEM, TGA, zeta potential, and a particle size analyzer. The effects of MMA/HEMA ratio, 5-FU, and MWCNTs contents on morphological and structural properties, trapping efficiency (EE%), and in-vitro drug release were studied. The obtained TEM images, XRD charts, and FTIR spectra demonstrate the efficient trapping of drugs in copolymeric and composite NPs. The existence of MWCNTs in the drug-loaded polymer enhances the stability against coagulation in the colloid system and the thermal stability. Also, the incorporation of MWCNTs increases the EE% to a high ratio (99% @ CNTs: drug ratio of 2:1) which permits loading of higher drug content. Also, 5-FU-loaded MWCNTs/copolymer nanocomposite exhibited a significant anti-proliferative effect against CaCo-2, MCF-7, and HepG-2 cell lines. Compared with the other two cell lines, it demonstrated stronger cytotoxicity against the HepG-2 cell line. Consequently, the optimized MWCNTs/copolymer nanocomposite would be a hopeful drug delivery system for the 5-FU drug.

Acknowledgements: We acknowledge stamatis douzinas scholarship titan cement Egypt (annual scholarship programme for graduates from beni suef and Alexandria) to pursue post graduate studies.

.

Compliance with ethical standards.

Conflict of interest: All authors declare that they have no conflict of interest.

Research involving human and animal participants: This article does not contain any studies with human or animal subjects performed by any of the authors.

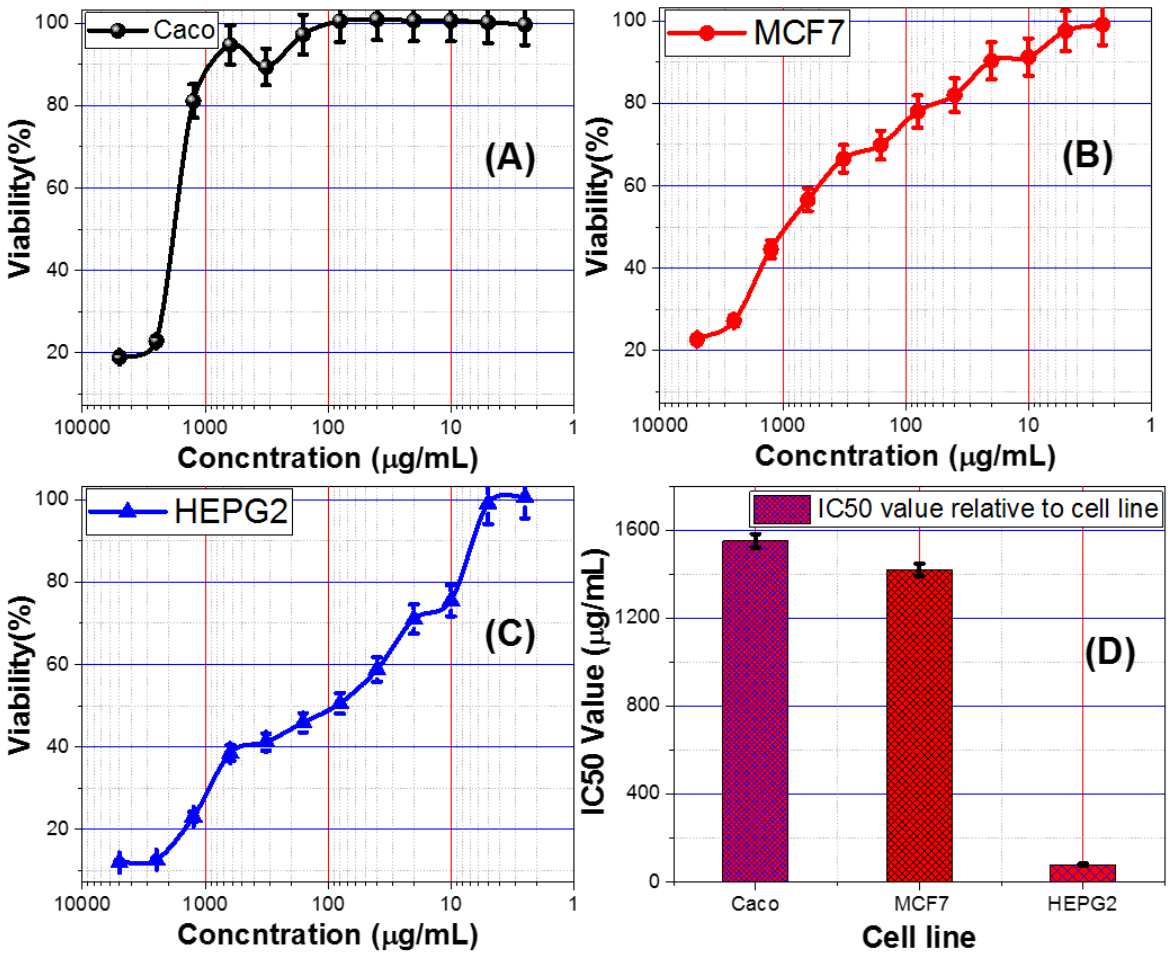

Figure 10: Anti-proliferative effect of the tested sample on (A)CaCo-2, (B)MCF-7, and (C)HepG-2cell lines in vitro; and (D) IC50 of the tested compound against different examined cell lines.

References

[1] Muslimov, A. R., Timin, A. S., Bichaykina, V. R., Peltek, O. O., Karpov, T. E., Dubavik, A., ... & Zyuzin, M. V. (2020). Biomimetic drug delivery platforms based on mesenchymal stem cells impregnated with light-responsive submicron sized carriers. *Biomaterials science*, *8*(4), 1137-1147.

[2] Moustafa, A. B., Sobh, R. A., Rabie, A. M., Nasr, H. E., & Ayoub, M. M. H. (2013). Synthesis and in vitro release of guest drugs- loaded copolymer nanospheres MMA/HEMA via differential microemulsion polymerization. *Journal of applied polymer science*, *129*(2), 853-865.

[3] Sobh, R. A., Mohamed, W. S., Moustafa, A. B., & Nasr, H. E. (2015). Encapsulation of curcumin and curcumin derivative in polymeric nanospheres. *Polymer-Plastics Technology and Engineering*, *54*(14), 1457-1467.

[4] Chanda, M. (2016). Direct Synthesis of Nano-size Polymers by Microemulsion Polymerization. In *Nano-size Polymers* (pp. 49-86). Springer, Cham.

[5] Majeed, A., Bashir, R., Farooq, S., & Maqbool, M. (2019). Preparation, characterization and applications of nanoemulsions: An insight. *Journal of Drug Delivery and Therapeutics*, *9*(2), 520-527.

[6] Sobh, R. A., Mohamed, W. S., Moustafa, A. B., & Nasr, H. E. (2015). Encapsulation of curcumin and curcumin derivative in polymeric nanospheres. *Polymer-Plastics Technology and Engineering*, *54*(14), 1457-1467.

[7] Moustafa, A. B., Sobh, R. A., Rabie, A. M., Nasr, H. E., & Ayoub, M. M. H. (2013). Differential microemulsion polymerization as a new root for entrapment of drugs. *Journal of applied polymer science*, *127*(6), 4634-4643.

[8] Moustafa, A. B., Sobh, R. A., Rabie, A. M., Nasr, H. E., & Ayoub, M. M. H. (2013). Synthesis and in vitro release of guest drugs- loaded copolymer nanospheres MMA/HEMA via differential microemulsion polymerization. *Journal of applied polymer science*, *129*(2), 853-865.

[9] Kumar, S., Rani, R., Dilbaghi, N., Tankeshwar, K., & Kim, K. H. (2017). Carbon nanotubes: a novel material for multifaceted applications in human healthcare. *Chemical society reviews*, *46*(1), 158-196.

[10] Mali, N. I. K. H. I. L., Jadhav, S., Karpe, M., & Kadam, V. I. L. A. S. R. A. O. (2011). Carbon nanotubes as carriers for delivery of bioactive and therapeutic agents: an overview. *International Journal of Pharmacy and Pharmaceutical Sciences*, *3*(3), 45-52.

[11] Hibino, N., Suzuki, S., Wakahara, H., Kobayashi, Y., Sato, T., & Maki, H. (2011). Short-wavelength electroluminescence from single-walled carbon nanotubes with high bias voltage. *ACS nano*, *5*(2), 1215-1222.

[12] Wei, G., Zhang, J., Xie, L., & Jandt, K. D. (2011). Biomimetic growth of hydroxyapatite on super water-soluble carbon nanotube-protein hybrid nanofibers. *Carbon*, *49*(7), 2216-2226.

[13] Nivethaa, E. A. K., Dhanavel, S., Rebekah, A., Narayanan, V., & Stephen, A. (2016). A comparative study of 5-Fluorouracil release from chitosan/silver and chitosan/silver/MWCNT nanocomposites and their cytotoxicity towards MCF-7. *Materials Science and Engineering: C*, *66*, 244-250.

[14] Wang, H., Li, J., Zhang, X., Ouyang, Z., Li, Q., Su, Z., & Wei, G. (2013). Synthesis, characterization and drug release application of carbon nanotube-polymer nanosphere composites. *RSC advances*, *3*(24), 9304-9310.

[15] Entezar-Almahdi, E., & Morowvat, M. H. (2019). Pharmacokinetic aspects of carbon nanotubes: improving outcomes of functionalization. *Current Nanoscience*, *15*(5), 454-459.

[16] González-Lavado, E., Valdivia, L., García-Castaño, A., González, F., Pesquera, C., Valiente, R., & Fanarraga, M. L. (2019). Multi-walled carbon nanotubes complement the anti-tumoral effect of 5-Fluorouracil. *Oncotarget*, *10*(21), 2022.

[17] Thomas, S. A., Grami, Z., Mehta, S., & Patel, K. (2016). Adverse effects of 5-fluorouracil: focus on rare side effects. *Cancer Cell & Microenvironment*, *3*.

[18] Farjadian, F., Ghasemi, A., Gohari, O., Roointan, A., Karimi, M., & Hamblin, M. R. (2019). Nanopharmaceuticals and nanomedicines currently on the market: challenges and opportunities. *Nanomedicine*, *14*(1), 93-126.

[19] Krishnaiah, Y. S. R., Satyanarayana, V., Kumar, B. D., Karthikeyan, R. S., & Bhaskar, P. (2003). In vivo pharmacokinetics in human volunteers: oral administered guar gum-based colon-targeted 5-fluorouracil tablets. *European Journal of Pharmaceutical Sciences*, *19*(5), 355-362.

[20] Entezar-Almahdi, E., Mohammadi-Samani, S., Tayebi, L., & Farjadian, F. (2020). Recent advances in designing 5-fluorouracil delivery systems: a stepping stone in the safe treatment of colorectal cancer. *International Journal of Nanomedicine*, *15*, 5445.

[21] Hassan, R. R. A., & Mohamed, W. S. (2017). Effect of methyl methacrylate/hydroxyethyl methacrylate copolymer on optical and mechanical properties and long-term durability of paper under accelerated ageing. *International Journal of Conservation Science*, *8*(2).

[22] Shaban, M., & Galaly, A. R. (2016). Highly sensitive and selective in-situ SERS detection of Pb 2+, Hg 2+, and Cd 2+ using nanoporous membrane functionalized with CNTs. *Scientific reports*, *6*(1), 1-9.

[23] Shaban, M., Ashraf, A. M., AbdAllah, H., & Abd El-Salam, H. M. (2018). Titanium dioxide nanoribbons/multi-walled carbon nanotube nanocomposite blended polyethersulfone membrane for brackish water desalination. *Desalination*, *444*, 129-141.

[24] Koukiotis, C., & Sideridou, I. D. (2008). Preparation of high solids stable translucent nanolatexes of MMA/BA copolymers and MMA/BA/Veova-10 terpolymers with low MFFT using green industrial surfactants. *Progress in Organic Coatings*, *63*(1), 116-122.

[25] Sobh, R. A., Nasr, H. E., Moustafa, A. B., & Mohamed, W. S. (2019). Tailoring of anticancer drugs loaded in MWCNT/Poly (MMA-co-HEMA) nanosphere composite by using in situ microemulsion polymerization. *Journal of Pharmaceutical Investigation*, *49*(1), 45-55.

[26] Sobh, R. A., Nasr, H. E. S., & Mohamed, W. S. (2019). Formulation and in vitro characterization of anticancer drugs encapsulated chitosan/multi-walled carbon nanotube nanocomposites. *Journal of Applied Pharmaceutical Science*, *9*(08), 032-040.

[27] Gopi, G., & Kannan, K. (2015). Fabrication and in vitro evaluation of nateglinide-loaded ethyl cellulose nanoparticles. *Asian J Pharm Clin Res*, *8*(6), 93-96.

[28] Thompson, C. J., Hansford, D., Higgins, S., Rostron, C., Hutcheon, G. A., & Munday, D. L. (2007). Evaluation of ibuprofen-loaded microspheres prepared from novel copolyesters. *International journal of pharmaceutics*, *329*(1-2), 53-61.

[29] Hashem, F. M., Abd Allah, F. I., Abdel-Rashid, R. S., & Hassan, A. A. (2020). Glibenclamide nanosuspension inhaler: development, in vitro and in vivo assessment. *Drug development and industrial pharmacy*, *46*(5), 762-774.

[30] Chu, H., Liu, N., Wang, X., Jiao, Z., & Chen, Z. (2009). Morphology and in vitro release kinetics of drug-loaded micelles based on well-defined PMPC–b–PBMA copolymer. *International journal of pharmaceutics*, *371*(1-2), 190-196.

[31] Valot, P., Baba, M., Nedelec, J. M., & Sintes-Zydowicz, N. (2009). Effects of process parameters on the properties of biocompatible ibuprofen-loaded microcapsules. *International journal of pharmaceutics*, *369*(1-2), 53-63.

[32] Lazaridou, M., Christodoulou, E., Nerantzaki, M., Kostoglou, M., Lambropoulou, D. A., Katsarou, A., ... & Bikiaris, D. N. (2020). Formulation and in-vitro characterization of chitosan-nanoparticles loaded with the iron chelator deferoxamine mesylate (DFO). *Pharmaceutics*, *12*(3), 238.

[33] Albalawi, A. M., Mohamed, W. S., & Elsayed, N. H. (2016). Utilization of MMT clay and MMT-Chitosan for platinol drug delivery. *Der Pharm Chem*, *8*(23), 27-34.

[34] Liu, L., Sun, L., Wu, Q., Guo, W., Li, L., Chen, Y., ... & Wei, Y. (2013). Curcumin loaded polymeric micelles inhibit breast tumor growth and spontaneous pulmonary metastasis. *International journal of pharmaceutics*, *443*(1-2), 175-182.

[35] Skehan, P., Storeng, R., Scudiero, D., Monks, A., McMahon, J., Vistica, D., ... & Boyd, M. R. (1990). New colorimetric cytotoxicity assay for anticancer-drug screening. *JNCI: Journal of the National Cancer Institute*, *82*(13), 1107-1112.

[36] Sianipar, M., Kim, S. H., Iskandar, F., & Wenten, I. G. (2017). Functionalized carbon nanotube (CNT) membrane: progress and challenges. *RSC advances*, *7*(81), 51175-51198.

[37] Masloub, S. M., Elmalahy, M. H., Sabry, D., Mohamed, W. S., & Ahmed, S. H. (2016). Comparative evaluation of PLGA nanoparticle delivery system for 5-fluorouracil and curcumin on squamous cell carcinoma. *Archives of oral biology*, *64*, 1-10.

[38] Anwer, M. K., Mohammad, M., Ezzeldin, E., Fatima, F., Alalaiwe, A., & Iqbal, M. (2019). Preparation of sustained release apremilast-loaded PLGA nanoparticles: in vitro characterization and in vivo pharmacokinetic study in rats. *International journal of nanomedicine*, *14*, 1587.

[39] Al-Osaimi, J., Alhosiny, N., Badawi, A., & Abdallah, S. (2013). The effects of CNTs types on the structural and electrical properties of CNTs/PMMA nanocomposite films. *Int J Eng Technol*, *13*, 77-79.

[40] Ashour, A. E., Badran, M., Kumar, A., Hussain, T., Alsarra, I. A., & Yassin, A. E. B. (2019). Physical pegylation enhances the cytotoxicity of 5-fluorouracil-loaded PLGA and PCL nanoparticles. *International journal of nanomedicine*, *14*, 9259.

[41] Peng, X., Zhuang, Q., Peng, D., Dong, Q., Tan, L., Jiao, F., & Liu, L. (2013). Sustained release of naproxen in a new kind delivery system of carbon nanotubes hydrogel. *Iranian journal of pharmaceutical research: IJPR*, *12*(4), 581.

[42] Hassan, R. R. A., & Mohamed, W. S. (2018). The impact of methyl methacrylate hydroxyethyl methacrylate loaded with silver nanoparticles on mechanical properties of paper. *Applied Physics A*, *124*(8), 1-10.

[43] Elbaz, N. M., Ziko, L., Siam, R., & Mamdouh, W. (2016). Core-shell silver/polymeric nanoparticles-based combinatorial therapy against breast cancer in-vitro. *Scientific reports*, *6*(1), 1-9.